International Journal of Signal Processing, Image Processing and Pattern Recognition
Vol.7, No.1 (2014), pp.299-312
http://dx.doi.org/10.14257/ijsip.2014.7.1.28

Analysis and Experimental Verification of Digital Self-Interference Cancelation for Co-time Co-frequency Full-Duplex LTE

Qiang Xu, Xin Quan, Zhiliang Zhang, Youxi Tang and Ying Shen

National Key Lab of Science and Technology on Communications, University of Electronic Science and Technology of China, 611731 Chengdu, China
xuqiang06@uestc.edu.cn, 15881069748@163.com, 13438133170@139.com, tangyx@uestc.edu.cn, shenying@uestc.edu.cn

Abstract

In the communication mechanism of co-time co-frequency full-duplex (CCFD), digital self-interference cancellation (SIC) is used for suppressing residual self-interference (SI) after antenna and radio frequency (RF) SICs, as well as low-power multipath SI. In this study, the CCFD LTE verification experiment is presented, which adopts digital SIC with the SI signal reconstructed in frequency domain. For the multipath Rayleigh SI channel, the expression of digital SIC capability is derived and the relationship among the channel estimation error, the received SI power, and digital SIC capability is analyzed. Experimental results show that the digital SIC ability is 31.2 dB for a 20 MHz 16QAM modulated LTE SI signal with frequency centered at 2.6 GHz and the interference-to-noise ratio of 40 dB.

Keywords: *Co-time Co-frequency Full-Duplex; Digital Self-interference; LTE*

1. Introduction

To improve the spectral efficiency of frequency division duplex or time division duplex system, theoretical analysis and preliminary experimental verification for co-time co-frequency full-duplex (CCFD) were carried out by industrial and academic scientists in recent years [1-3]. Researches have shown that CCFD allows the transmitter and the receiver of an equipment work simultaneously using the same frequency. Therefore, uplink and downlink of wireless communication can use the same frequency resource simultaneously. In theory, CCFD can double the spectral efficiency [4].

As the transmitter and the receiver work simultaneously at the same frequency, the transmitted signal of CCFD transmitter will cause strong interference to the local receiver. Therefore, the critical step of CCFD design is to suppress the strong self-interference (SI) [1, 3]. Studies on self-interference cancellation (SIC) carried out in recent years can be categorized as antenna SIC [5, 6], radio frequency (RF) SIC [7-9], and digital SIC [3, 10-12]. Among them, the antenna SIC and the RF SIC are implemented in the analog domain. They are used to eliminate the line of sight (LOS) SI [7] and some strong multipath SI [13], ensuring the received signal could pass the analog to digital converter (ADC). The performance of the cancellation is related to SI signal bandwidth, adjustment error, RF channel non-ideal characteristics, and equipment environment change [14, 15]. After RF SIC, digital SIC is performed in the digital domain, as an important composition part of SIC. It can significantly suppress the residual multipath SI, some low-power multipath SI, and the residual SI caused by the RF adjustment error and environmental changes [15].

Digital SIC scheme can be accomplished by employing SI signal reconstructing [10, 12, 16], adaptive filtering [3, 17] and pre-coding [4, 18], and has some preliminary engineering

ISSN: 2005-4254 IJSIP

verification [1, 4, 7]. Among them, a typical SI reconstructing digital SIC scheme is given in [7] and [16]. In [7], RF SIC and digital SIC were used sequentially to reduce the SI power. Digital SIC was carried out in three steps, *i.e.*, (1)using the least squares (LS) method to perform channel estimation, (2)reconstructing the SI signal in time domain by employing channel estimation and the digital transmitted signal, (3)subtracting the reconstructed SI signal from the received signal. For a 10 MHz WiFi SI signal with the received power varying from −30 dBm to −10 dBm, the digital SIC capability was about 30 dB. The experiment verified the digital SIC capability at high interference-to-noise ratio (INR), however it did not reflect the relationship between digital SIC capability and received SI power. And the effect of channel estimation error on the digital SIC capability was not considered. In [16], SIC scheme was organized by, (1)generating the digital cancelling signal by employing the channel estimation and digital transmitted signal in the frequency domain, (2)transmitting the digital cancelling signal through the RF path to obtain the RF cancelling signal, (3)subtracting the RF cancelling signal and digital cancelling signal sequentially from the received signal to accomplished RF and digital SICs. The experiments examined the RF SIC capability and the joint cancellation capability under different received SI power. For a 10 MHz WiFi SI signal, the maximum joint cancellation was 36 dB. Due to the limitation of the SIC scheme, the digital SIC capability changed with the RF SIC capability. Besides, the experiment lacked the independent verification of the digital SIC capability. Therefore, the relationship among the received SI power, the channel estimation error, and the digital SIC capability needs to be explored and experimentally verified.

In this study, the CCFD LTE verification experiment is presented, which adopts digital SIC with the SI signal reconstructed in frequency domain after applying RF SIC proposed in [7]. Under the condition of multipath SI Rayleigh channel, the systematic scheme and the cancellation capability of the digital SIC used in experiment are analyzed. A closed-form expression for digital SIC capability is derived in terms of the received SI power and the SI channel estimate error. Simulation and experimental curves are presented to show that the digital SIC capability decreases with the increase of channel estimation error, and increases with the rising of received SI power. The trends and differences among these curves are also analyzed.

The rest of this paper is arranged as follows. Section 2 gives the systematic scheme of digital SIC in our experiment, and then presents the error analysis and theoretical and simulation results. Section 3 introduces the platform, procedure, and key algorithm used in the experiment. Section 4 gives experimental results and analyzes the difference between experimental and simulation results. Section 5 is the summary.

2. Principle of Experiment Design

2.1. Systematic Scheme

An OFDM-based CCFD single-input single-output (SISO) system is shown in Figure 1, where denotes the carrier frequency. Take the local equipment as an example. Since the transmitter and the receiver work at the same time and the same frequency, the receiver hears not only the desired signal $r_U(t)$ from the remote equipment, but also the SI signal $r_I(t)$ from its transmitter. Therefore, it is essential to cancel SI signal. To improve the SIC performance, we employ both RF SIC and digital SIC to reduce SI power. RF SIC aims to eliminating high-power LOS SI, and digital SIC eliminates the residual multipath SI. In this paper, we focus on the digital SIC, and the RF SIC can be found in [14].

According to the analysis above, the signal $r(t)$ received by the local receiver is:

$$r(t) = r_U(t) + r_I(t) + n(t) \tag{1}$$

where $r_U(t)$, $r_I(t)$, $n(t)$ are the desired signal, the SI signal, and the white Gaussian noise, respectively.

As there is a LOS path between the transmit antenna and the receive antenna, the SI channel response is modeled as Rice channel, thus the SI signal $r_I(t)$ can be expressed as:

$$r_I(t) = a_0^I(t)s_I(t - t_0^I) + \sum_{l=1}^{L_I} a_l^I(t)s_I(t - t_l^I) \tag{2}$$

where $s_I(t)$ is the local transmitted signal and L_I is the multipath number of the SI channel. $a_0^I(t)$ and t_0^I are the attenuation factor and delay of LOS path at time t, respectively. $a_l^I(t)$ and t_l^I are the attenuation factor and delay of the l path at time t, respectively.

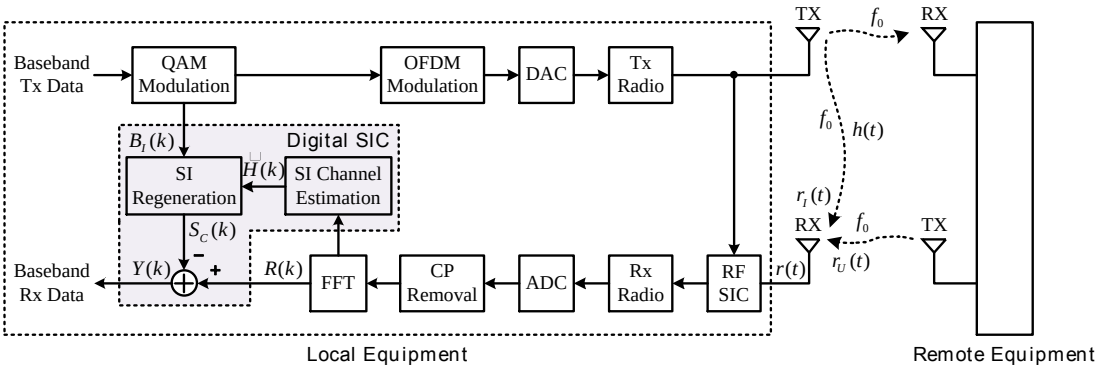

Figure 1. Systematic Scheme of Digital SIC in SISO CCFD System

Because most of the LOS SI power can be reduced by RF SIC, the SI channel impulse response after RF SIC can be modeled as Rayleigh channel, and thus the residual SI after RF SIC is:

$$r_{DI}(t) = \sum_{l=1}^{L_I} a_l^I(t)s_I(t - t_l^I) \tag{3}$$

After applying sequentially the analog-to-digital, cyclic prefix (CP) removal, and fast Fourier transform (FFT), the digital frequency domain received signal is obtained, where the symbol at the *k*-th subcarrier is

$$R(k) = R_U(k) + R_I(k) + N(k) \tag{4}$$

with $R_U(k)$, $R_I(k)$, and $N(k)$ the digital frequency domain symbols of $r_U(t)$, $r_{DI}(t)$, and $n(t)$, respectively. Supposing the subcarrier number of the system is M and each subcarrier has the equal power, after ideal synchronization, $R_I(k)$ and $R_U(k)$ can be expressed as

$$R_I(k) = \sqrt{\frac{E_{SI}}{M}} H_I(k)B_I(k) \tag{5}$$

$$R_U(k) = \sqrt{\frac{E_{SU}}{M}} H_U(k) B_U(k) \tag{6}$$

where E_{SI} and E_{SU} are the transmit power and desired signal power, respectively. $H_I(k)$ and $H_U(k)$ are the frequency domain channel response of the *k*-th subcarrier of the SI channel and the desired signal channel, respectively. $B_I(k)$ and $B_U(k)$ are the frequency domain transmitted signal of the kth subcarrier of the SI signal and the desired signal, respectively.

Digital SIC is accomplished by employing the frequency domain reconstructed SI signal [7]. As shown in Figure 1, it consists of three components. First, apply SI channel estimation to obtain the frequency domain channel response $\hat{H}(k)$. Then, employ the channel estimation $\hat{H}(k)$ and the frequency domain transmitted signal $B_I(k)$ to obtain the frequency domain reconstructed self-interference signal $S_C(k)$,

$$S_C(k) = \sqrt{\frac{E_{SI}}{M}} \hat{H}(k) B_I(k) \tag{7}$$

Finally, subtract the reconstructed SI signal $S_C(k)$ from $R(k)$ in the frequency domain to obtain the digital signal $Y(k)$ after digital SIC. Thus $Y(k)$ is expressed as

$$Y(k) = R(k) - S_C(k) = R_U(k) + R_r(k) + N(k) \tag{8}$$

where $R_r(k)$ is the residual SI symbol after digital SIC:

$$R_r(k) = R_I(k) - S_C(k) = \sqrt{\frac{E_{SI}}{M}} \left(H(k) - \hat{H}(k) \right) B_I(k) \tag{9}$$

The performance of the digital SIC can be measured by the digital SIC capability G (dB) [14], which is defined as:

$$G = 10 \lg \frac{E_I + s^2}{E_r + s^2} \tag{10}$$

where E_I is the power of the SI symbol $R(k)$ before digital SIC, and E_r is the power of residual SI symbols $R_r(k)$ after digital SIC.

2.2. Error Analysis

From Eq. (9), it can be seen that after ideal synchronization, the residual SI signal is determined by SI channel estimation $\hat{H}(k)$, thus the accuracy of $\hat{H}(k)$ is the key factor influencing the digital SIC capability.

According to Eq. (9), the power of residual SI E_r is:

$$\begin{aligned} E_r &= E\left\{\left|\sqrt{\frac{E_{SI}}{M}}\left(H(k)-\hat{H}(k)\right)B_I(k)\right|^2\right\} \\ &= \frac{E_{SI}}{M}E\left\{\left|H(k)-\hat{H}(k)\right|^2\right\} \\ &= \frac{gE_{SI}}{M} \end{aligned} \tag{11}$$

where g is the mean square error (MSE) of channel estimation defined as

$$g = E\left\{\left|\hat{H}(k)-H(k)\right|^2\right\} \tag{12}$$

It can be seen that E_r is a function of the transmitted SI power E_{SI} and the MSE of channel estimation g.

Substituting Eq. (11) into Eq. (10), we have the digital SIC capability :

$$G = 10\lg\frac{E_I + s^2}{\frac{gE_{SI}}{M} + s^2} = 10\lg\frac{R_{IN}+1}{g'R_{IN}+1} \tag{13}$$

where R_{IN} is the interference-to-noise ratio (INR), i.e., the power ratio of the SI signal before digital SIC and the thermal noise, and can be expressed as

$$R_{IN} = \frac{E_I}{s^2} \tag{14}$$

g' is the normalized mean square error (NMSE) of channel estimation, defined as

$$g' = \frac{g}{E\left\{\left|H_I(k)\right|^2\right\}} \tag{15}$$

We also analyze the influence of residual SI on the desired signal demodulation. After digital SIC, the desired signal-to-interference and noise ratio is R_{SIN},

$$R_{SIN} = \frac{E_U}{\frac{gE_{SI}}{M} + s^2} = \frac{R_{IN}}{g'R_{IN}R_{IS} + R_{IS}} \tag{16}$$

where R_{IS} is the power ratio of the SI signal and the desired signal before digital SIC:

$$R_{IS} = \frac{E_I}{E_U} \tag{17}$$

According to the bit error rate (BER) function of 16QAM under Rayleigh channel [19], the demodulation BER of the desired signal is:

$$P_e = \frac{1}{4}\left\{1.5\left(1-\sqrt{\frac{R_{SIN}}{2.5+R_{SIN}}}\right)-\frac{9}{16}\left[1-\sqrt{\frac{R_{SIN}}{2.5+R_{SIN}}}\left(\frac{4}{p}\arctan\sqrt{\frac{2.5+R_{SIN}}{R_{SIN}}}\right)\right]\right\} \quad (18)$$

2.3. Theoretical and Simulation Results

On the basis of Sections 2.1 and 2.2, this section presents theoretical analysis and simulation verification to measure the influence of the channel estimation error and the received SI power on digital SIC capability and BER of the desired signal. Parameters used in analysis and simulations are shown in Table 1.

Table 1. Analysis and Simulation Parameters

Theoretical analysis parameters	Modulation mode	16QAM
	Desired signal channel	Rayleigh channel
	SI channel	Rayleigh channel
	Desired signal power	−68 dBm
	Thermal noise power	−98 dBm
	Received SI power (dBm)	−88,−78, −68, −58, −48
	SI channel estimation NMSE	0, 10^{-4}, 10^{-3}, 10^{-2}, 10^{-1}
Simulation parameters	OFDM subcarrier number	2048
	Modulation mode	16QAM
	IFFT length	2048
	Signal bandwidth	20 MHz
	Desired signal channel	Rayleigh channel
	SI channel	Rayleigh channel
	SNR	30 dB
	INR (dB)	10, 20, 30, 40, 50
	SI channel estimation NMSE	0, 10^{-4}, 10^{-3}, 10^{-2}, 10^{-1}
	Desired signal channel estimation	Ideal estimation

According to Eq. (13), the relationship between the digital SIC capability and the received SI power can be obtained different SI channel estimation NMSE. Theoretical and simulation results are shown in Figure 2 with the SI channel estimation NMSE ranging from 0 to 10^{-1}. The simulation curve matches well with the theoretical curve. It can be seen that:

(1) For a specific NMSE, the digital SIC capability G increases with the increase of the received SI power and finally reaches an upper bound. The upper bound can be explained by obtain the limit of as R_{IN} approaches infinity.

$$G_{\lim} = \lim_{INR\to\infty} 10\lg\frac{R_{IN}+1}{g'R_{IN}+1} = -10\lg g' \quad (19)$$

It can be seen that the upper bound of the digital SIC capability is only related to the SI channel estimation NMSE.

(2) For a given received SI power, *i.e.*, INR R_{IN} is fixed, the digital SIC capability G decreases as the SI channel estimation NMSE increases.

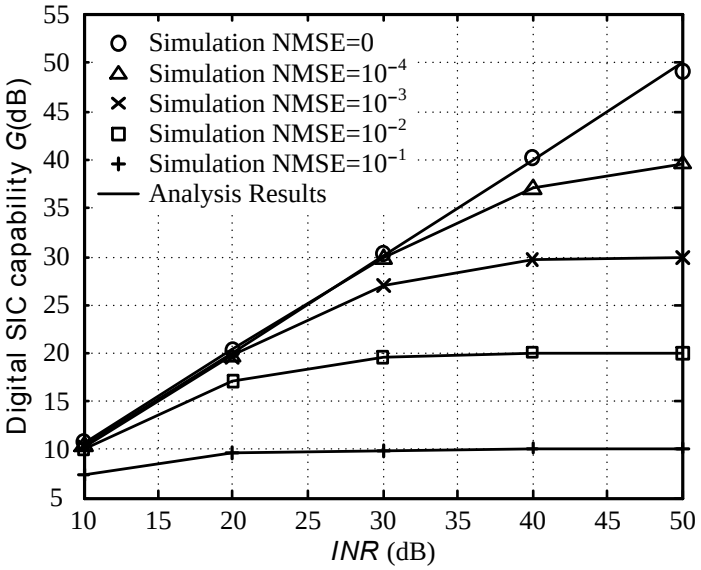

Figure 2. Digital SIC Capability versus the Received SI Power

According to Eqs. (16) and (18), the relationship between the demodulation BER of the desired signal and the received SI power can be obtained. The theoretical and simulation results are shown in Figure 3 with the SI channel estimation NMSE ranging from 0 to 10^{-1}. It can be seen that:

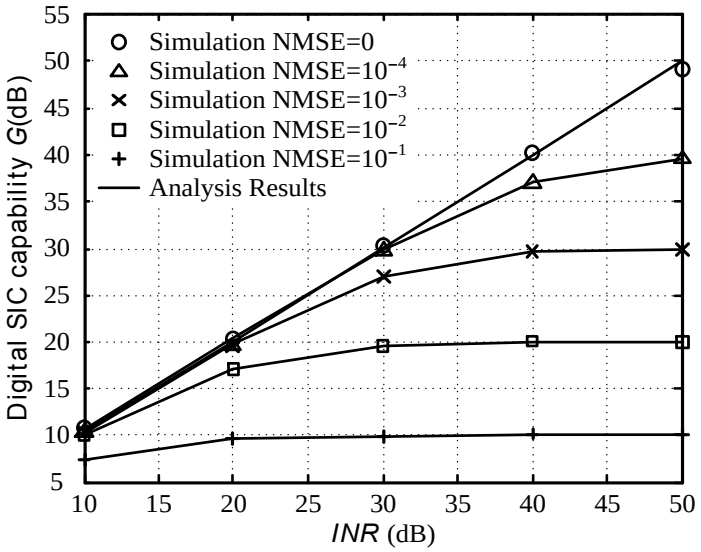

Figure 3. Demodulation BER of the Desired Signal versus the Received SI Power

(1) For a specific SI channel estimation NMSE, the demodulation BER increases with the increase of the received SI power, which indicates that a stronger SI produces a larger impact on the desired signal demodulation.

(2) For a given INR R_{IN}, the demodulation BER increases as the SI channel estimation NMSE increases.

3. Experimental Verification Scheme

We built a test platform to experiment the validity of the digital SIC scheme and the effect of the SI channel estimation error and the received SI power on digital SIC.

3.1. Experimental Platform and Environment

The experiments were accomplished indoors using the test platform we built. The experimental environment is shown in Figure 4, and some key parameters of the platform are shown in Table 2.

(a) Panorama (b) Enlarged Details

Figure 4. Experimental Environment

Table 2. Key Parameters

Parameter	Indicator
Antenna configuration	SISO
Modulation mode	16QAM+OFDM
Signal bandwidth	20 MHz
Transmit intermediate frequency	122.88 MHz
DA bits	16
DA sampling rate	491.52 MHz
RF carrier frequency	2.6 GHz
Receive intermediate frequency	153.6 MHz
AD nominal number of bits	14
AD effective number of bits	12
AD sampling rate	122.88 MHz

3.2. Experiment Procedure

Our goal is to verify the validity of digital SIC and the impact of the received SI power on the digital SIC capability and the demodulation BER of the desired signal. To improve the SIC performance, we employ both RF SIC and digital SIC to reduce SI power. The experiments are organized as follows.

(1) Record the power of noise without the SI signal or the desired signal.

(2) Make the remote equipment transmit signals and adjust the transmitting power to ensure the SNR after ADC equal 30 dB.

(3) Stop the remote equipment transmitting.

(4) Make the local equipment transmit signals and adjust the transmitting power to ensure the INR after ADC equal 10dB.

(5) Record the difference G_1 between the power before and after digital SIC.

(6) Make the remote equipment transmit and record the demodulation BER P_{e1}.

(7) Adjust the local equipment transmitting power to set the INR equal 14, 20, 27, 30, 34, and 40 dB, respectively, repeat (3) to (6), and record the digital SIC capability G_i and the demodulation BER P_{ei} under different INR.

3.3. Key Algorithms

The key algorithms in experiments include the synchronization algorithm and the SI channel estimation algorithm. A brief introduction is listed as follows.

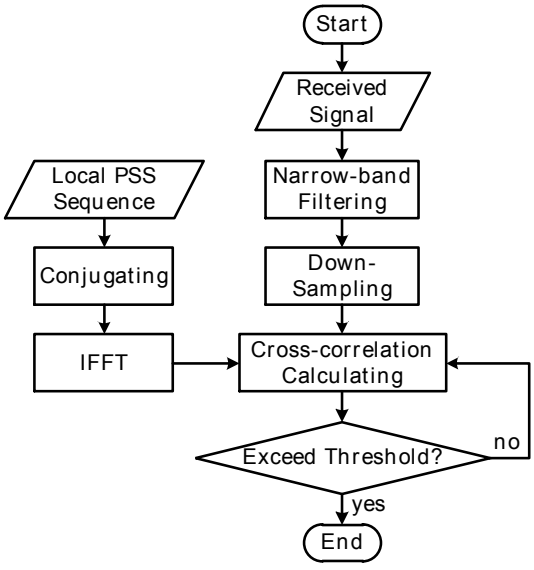

Figure 5. The SI Signal Synchronization in CCFD Experiments

3.3.1. Synchronization: In the 3GPP LTE protocol, a primary synchronization signal (PSS) sequence, which is generated by a Zadoff Chu (ZC) sequence, has an excellent autocorrelation and cross-correlation properties. Thus, the local equipment and the remote

equipment adopt different PSS sequences in the experiments, and cross-correlation algorithm is used to synchronization.

The process of synchronization is shown in Figure 5. After the received signal is filtered and downsampled, it takes sliding correlation with the local PSS sequence. Synchronization is completed when the correlation result exceed the threshold. Otherwise, synchronization continues.

3.3.2. SI Channel Estimation: We use the LS algorithm to obtain the SI channel estimation by exploiting the reference signal in frequency domain. The algorithm is implemented as

$$\hat{H}(k) = \frac{Y(k)}{X(k)} \tag{20}$$

where $Y(k)$, $X(k)$, and $\hat{H}(k)$ are the received reference signal, the transmitted reference signal, and channel estimation in frequency domain, respectively.

4. Experimental Results and Analysis

4.1. Experimental Results

The curves of the digital SIC capability and the BER of the desired signal are shown in Figure 6 and Figure 7, with a SNR of 30dB and the received SI power varying from 10 dB to 40 dB. Comparing experimental curves with simulation curves, it can be seen that:

(1) Experimental curves have the same trend with simulation curves. Both digital SIC capability and the BER of the desired signal increase with the increase of the received SI power, and digital SIC capability tends to an upper bound.

(2) Experimental results with the INR varying from 10 dB to 30 dB quite match simulation results with NMSE varying from 10^{-1} to 10^{-3}, correspondingly. While there's a significant gap between the experimental result with the INR of 40 dB and the simulation result with NMSE of 10^{-4}.

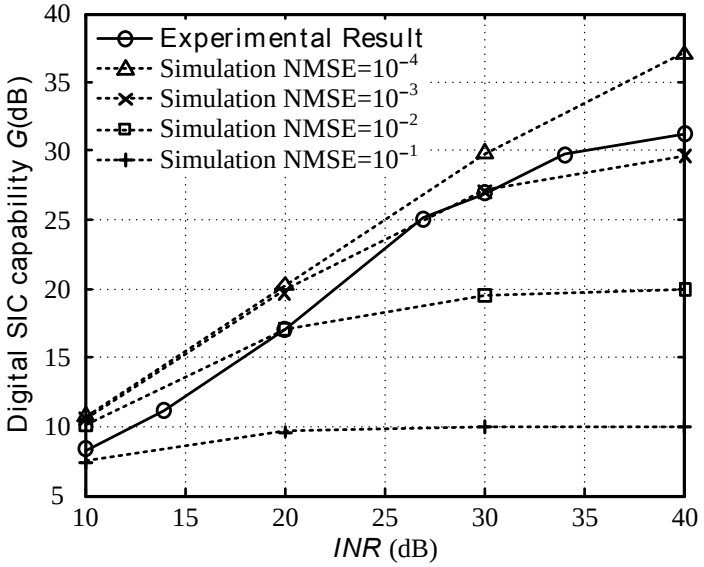

Figure 6. Digital SIC Capability versus the Received SI Power

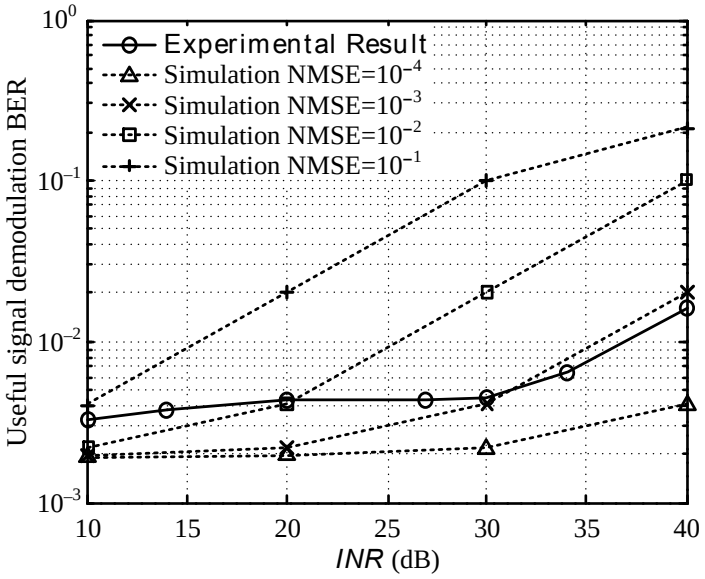

Figure 7. BER of the Desired Signal versus the Received SI Power

The SI signal spectra before and after digital SIC with the INR of 30 dB are shown in Figure 8, where the SI power is normalized to noise power. The SI spectrum fluctuates before digital SIC, whereas it becomes relatively even with an INR of 3.15 dB after digital SIC. It can be concluded that the digital SIC capability is about 26.85 dB, and digital SIC effectively improves the unevenness in the spectrum caused by RF SIC.

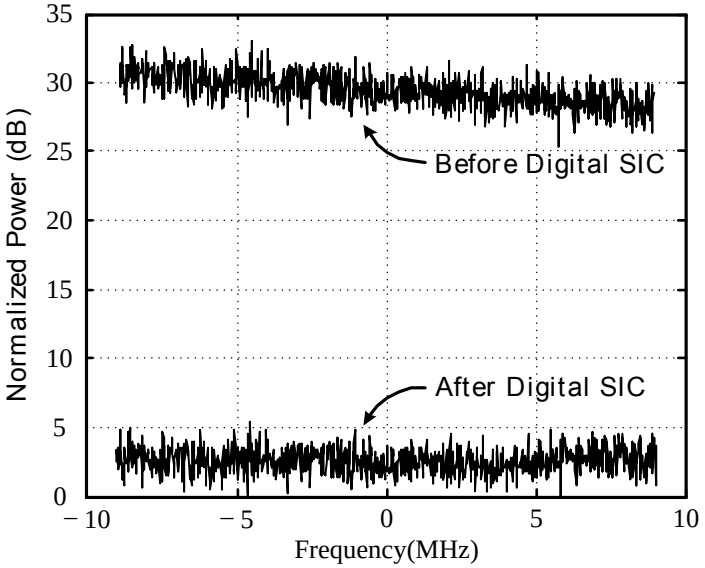

Figure 8. Signal Spectra before and after Digital SIC with INR of 30 dB

4.2. Comparison and Analysis

Some analysis on the difference between experimental results and simulation results are given as follows. In experiments, the SI channel estimation is obtained by employing LS algorithm. Using Eq.(20), we have

$$\hat{H}(k) = H(k) + \frac{N(k)}{X(k)} \tag{21}$$

Substituting Eq. (21) into Eq. (15), the LS channel estimation NMSE can be obtained as

$$g' = E\left\{\left|\frac{N(k)/X(k)}{H(k)}\right|^2\right\} = \frac{s^2}{E_I} = \frac{1}{R_{IN}} \tag{22}$$

According to Eq. (22), the SI channel estimation NMSE is 10^{-1}, 10^{-2}, 10^{-3} and 10^{-4} with INR varying from 10 dB to 40 dB, respectively. Therefore, experimental results with the INR lower than 30 dB quite match simulation results. While in the case of INR being 40 dB, the experimental result is dramatically different with the simulation result when NMSE is 10^{-4}. The major reason of the dramatic difference is that, in the case of high INR, non-ideal factors such as phase noise and amplifier nonlinearity, dominantly influence the digital SIC and thus the demodulation BER of the desired signal.

5. Conclusion

In this paper, we designed the CCFD LTE verification experiment by adopting the digital SIC with the SI signal reconstructed in frequency domain. Under the condition of multipath SI Rayleigh channel, the closed-form expression for digital SIC capability was derived. Simulation and experimental curves were presented to show that, the digital SIC capability decreases with the increase of the channel estimation error, and increases with the rising of the received SI power. The analysis and experimental results in this paper provided theoretical guidance for the algorithm selection and optimization in digital SIC, and the reference data for CCFD LTE engineering application.

Acknowledgements

This work was supported in part by the National Science Foundation of China (under grant NO. 61271164, U1035002/L05, 61001087, and 61101034), the National Science and Technology Major Project (under grant NO. 2014ZX03003001-002, 2012ZX03003010-003, and 2011ZX03001-006-01)

References

[1] M. Duarte and A. Sabharwal, “Full-duplex Wireless Communication Using Off-the Shelf Radios: Feasibility and First Results”, Conference Record of the Forty Fourth Asilomar Conference on Signals, Systems and Computers, California, USA, **(2010)** November 7-10.
[2] A. Sahai, G. Patel and A. Sabharwal, “Pushing the Limits of Full-Duplex: Design an Real-time Implementation”, The Computing Research Repository, **(2010)**.
[3] R. Lopez-Valcarce, E. Antonio-Rodriguez, C. Mosquera and F. Perez-Gonzalez, “An Adaptive Feedback Canceller for Full-Duplex Relays Based on Spectrum Shaping”, IEEE Journal on Selected Areas in Communications, vol. 30, **(2012)**, pp. 1566-1577.
[4] Y. Hua, P. Liang, Y. Ma and A. C. Cirik, “A Method for Broadband Full-Duplex MIMO Radio”, IEEE Signal Processing Letters, vol. 19, **(2012)**, pp. 793-796.

[5] J. I. Choi, M. Jain, K. Srinivasan, P. Levis and S. Katti, "Achieving Single Channel, Full Duplex Wireless Communication", MobiCom '10 Proceedings of the 17th annual international conference on Mobile computing and networking, Illinois, USA, **(2010)** September 20-24.
[6] M. A. Khojastepour, K. Sundaresan, S. Rangarajan, X. Zhang and S. Barghi, "The Case for Antenna Cancellation for Scalable Full-Duplex Wireless Communications", 10th ACM Workshop on Hot Topics in Networks, Massachusetts, UK, **(2011)** November 14-15.
[7] M. Jain, J. I. Choi, T. Kim, D. Bharadia, S. Seth, K. Srinivasan, P. Levis, S. Katti and P. Sinha, "Practical, Real-time, Full Duplex Wireless", MobiCom '11 Proceedings of the 17th annual international conference on Mobile computing and networking, Nevada, USA, **(2011)** September 19-23.
[8] S. Hong, J. Mehlman and S. Katti, "Picasso: Flexible RF and Spectrum Slicing", Proceedings of the ACM SIGCOMM 2012 conference on Applications, technologies, architectures, and protocols for computer communication, Helsinki, Finland, **(2012)** August 13-17.
[9] M. E. Knox, "Single Antenna Full Duplex Communications using a Common Carrier", 2012 IEEE 13th Annual Wireless and Microwave Technology Conference, Florida, USA, **(2012)** April 15-17.
[10] Y. J. Lee, J. B. Lee, S. I. Park, Y. T. Lee, H. M. Kim and H. N. Kim, "Feedback Cancellation for T-DMB Repeaters based on Frequency-domain Channel Estimation", IEEE Transactions on Broadcasting, vol. 57, **(2011)**, pp. 114-120.
[11] Y. Liu, X. Xia and H. Zhang, "Distributed Space-Time Coding for Full-Duplex Asynchronous Cooperative Communications", IEEE Transactions on Wireless Communications, vol. 11, **(2012)**, pp. 2680-2688.
[12] D. Chang, "Apparatus and Method for Removing Self-Interference and Relay System for the Same", U.S. Patent US8224242B2, **(2012)** June 17.
[13] J. G. McMichael, K. E. Kolodziej, "Optimal tuning of analog self-interference cancellers for full-duplex wireless communication", 2012 50th Annual Allerton Conference on Communication, Control, and Computing, Illinois, USA, **(2012)** October 1-5.
[14] Q. Xu, X. Quan, W. Pan, S. Shao and Y. Tang, "Analysis and Experimental Verification of RF Self-Interference Cancelation for Co-time Co-frequency Full-Duplex LTE", Journal of Electronics & Information Technology, to appear, **(2013)**.
[15] G. R. Kenworthy, "Self-cancelling full-duplex RF communication system", U.S. Patent US5681978, **(1997)** November 25.
[16] M. Duarte, C. Dick and A. Sabharwal, "Experiment-driven Characterization of Full-Duplex Wireless Systems", IEEE Transactions on Wireless Communications, vol. 11, **(2012)**, pp. 4296-4307.
[17] C. C. Tung, "Full Duplex Wireless Method and Apparatus", U.S. Patent US20120263078A1, **(2012)** October 18.
[18] D. Choi and D. Park, "Effective self-interference cancellation in full duplex relay systems", Electronics Letters, vol. 48, **(2012)**, pp. 129-130.
[19] M. K. Simon and M. S. Alouini, "Digital communication over fading channels", John Wiley & Sons, New York, **(2000)**, pp. 221.

Authors

Qiang Xu was born in Sichuan, China, in 1983. He received the B.E. degree in Communication and Information Engineering from the University of Electronic Science and Technology of China, Chengdu, China, in 2006 and the M.S. degrees in communications and information systems from the University of Electronic Science and Technology of China, Chengdu, China, in 2009. Since 2009, he has been with the National Key Laboratory of Science and Technology on Communications, University of Electronic Science and Technology of China, as an Assistant Lecturer. His general research interests include hardware and software design for communications that touch the physical world, and wireless mobile systems with emphasis on signal processing in communications.

Xu Qiang was born in Hebei, China, in 1988. She received the B.E. degree in Electronic and Information Engineering from Yanshan University in 2010. She is currently pursuing the Ph.D. in communication and information systems at the University of Electronic Science and Technology of China, Chengdu, China. Her research interests include full-duplex communication and signal processing.

Zhiliang Zhang was born in Guangdong, China, in 1981. He received the B.E. degree in electronic information science and technology and M.S. degree in circuits and systems from the Sichuan University, Chengdu, China, in 2003 and 2006, respectively. Since 2010, he has been working toward the Ph.D. degree in communications and information systems at the University of Electronic Science and Technology of China, Chengdu, China. His general research interests include full-duplex communication and signal processing.

Youxi Tang, is a professor with the National Key Laboratory of Science and Technology on Communications, University of Electronic Science and Technology of China. He received the B.E. degree in radar engineering from College of PLA Ordnance, in 1985 and the M.S. and Ph.D. degrees in communications and information systems from the University of Electronic Science and Technology of China, in1993 and 1997, respectively. He His research interests include spread spectrum systems and wireless mobile systems with emphasis on signal processing in communications

Ying Shen received the BS, MS, and PhD degrees in communications and information systems from the University of Electronic Science and Technology of China, Chengdu, China, in 2002, 2006, and 2009, respectively. Currently, he is working at the National Key Laboratory of Science and Technology On Communications, University of Electronic Science and Technology of China, Chengdu, China. His research interests include cognitive radio, MIMO and broadcasting systems.